Eur. Phys. J. D **14**, 331–335 (2001)

THE EUROPEAN PHYSICAL JOURNAL D

EDP Sciences

Influence of laser pulse width on absolute EUV-yield from Xe-clusters

M. Schnürer[1,a], S. Ter-Avetisyan[1,2], H. Stiel[1], U. Vogt[1], W. Radloff[1], M. Kalashnikov[1], W. Sandner[1], and P.V. Nickles[1]

[1] Max-Born-Institut, Max-Born-Str. 2a, 12489 Berlin, Germany
[2] Institute for Physical Research, 378410 Ashtarak-2, Armenia

Received 11 January 2001 and Received in final form 27 March 2001

Abstract. Using 50 fs ($\sim 2 \times 10^{18}$ W/cm^2) and 2 ps ($\sim 5 \times 10^{16}$ W/cm^2) pulses from a Ti:Sa multi-TW laser at 800 nm wavelength large Xe-clusters (10^5...10^6 atoms per cluster) have been excited. Absolute yield measurements of EUV-emission in a wavelength range between 10 nm and 15 nm in combination with cluster target variation were carried out. The ps-laser pulse has resulted in about 30% enhanced and spatially more uniform EUV-emission compared to fs-laser excitation. Circularly polarized laser light instead of linear polarization results in enhanced emission which is probably caused by electrons gaining higher energies by the polarization dependent optical field ionization process. An absolute emission efficiency at 13.4 nm of up to 0.8% in 2π sr and 2.2% bandwidth has been obtained.

PACS. 52.38.Ph X-ray, γ-ray and particle generation – 52.50.Jm Plasma production and heating by laser beams (laser-foil, laser-cluster, etc.) – 36.40.Vz Optical properties of clusters

Bright and compact radiation sources in the EUV-region are currently looked for key technologies and intriguing applications, such as EUV lithography, spectroscopy, metrology and microscopy [1–3]. Because several of these applications relay on sufficient average radiation power a laser driven source should advantageously use renewable and low debris EUV-emission targets like gaseous or liquid media. Instead of pure atomic gases for a medium consisting of "van der Waals" bonded rare gas assemblies of up to 10^7 atoms (clusters) a much higher laser absorption [4] could be demonstrated at intensities necessary to produce a plasma as a strong EUV-radiation emitter. This fact is attributed to a deposition of a large amount of laser energy in a small volume of these clusters during laser pulse widths similar or shorter to its disassembly time. Meeting this condition several work was devoted to the emission of short wavelength light in the spectral range of the EUV [5] up to hard X-rays [6]. Moreover the release of energetic ions from exploding clusters [7,8] has been analyzed in context to different excitation mechanisms [5,9].

In this paper we investigate the absolute emission of Xe-clusters with two different laser pulse widths and polarizations in the spectral region between 10 nm and 15 nm which is currently under intensive investigation for lithographic [1,10,11] technologies. Different heating laser pulse widths within the disassembly time window of clusters have not been applied for Xe-clusters in context to EUV-emission so far (for Ar- and Kr-clusters see [12]) as well as laser polarization and target characteristics have been not or only limited looked at (see *e.g.* [13]). In general there is only little work on reliable absolute emission data from different Xe-aggregations, whereby Xe is strongly anticipated as as laser driven EUV-source [14].

The experiments have been carried out with 50 fs and 2 ps laser pulses at 800 nm center wavelength from a 10 Hz repetition rate multi-TW Ti:Sa laser [15]. A 200 mJ beam of 60 mm in diameter is focused with a $f/2.5$ off axis parabolic mirror. Interaction intensities of $\sim 2 \times 10^{18}$ W/cm^2 (50 fs) and of $\sim 5 \times 10^{16}$ W/cm^2 (2 ps) have been estimated (see also [16]). From second order harmonic conversion and autocorrelation experiments we conclude that a ns-pulse pedestal produces not higher intensities than 10^{13} W/cm^2 in the focus and that the two pulses differ definitely in the pulse peak ± 2 ps window. The role of the prepulse in cluster heating was recently studied by Auguste *et al.* [17].

The Xe-cluster target was formed by expanding Xe gas from pressures up to 55 bar and a temperature of $T_0 = 300$ K through a supersonic conical nozzle with a cone angle $2\theta = 7°$, throat diameter of 400 μm and an 8 mm long conical section. From our parameter set already at 5 bar a condensation scaling parameter Γ^* of Hagena [18] $\Gamma^* \geq 10^5$ results from which one can expect large cluster formation. The cluster beam is pulsed by an electromagnetic valve for every 3 s with a pulse duration of 5 ms which keeps the background pressure before each gas pulse on a 10^{-6} mbar level. The laser focus is

[a] e-mail: schnuerer@mbi-berlin.de

placed approximately 1 mm below the orifice of the nozzle. Soft X-ray spectra were measured simultaneously at different angles relative to the incident laser beam axis. One transmission grating spectrometer (TGS, on-axis) is looking at the target along the laser beam in axial direction (grating 2 000 l/mm, resolution $\lambda/\Delta\lambda = 60$ at 13 nm) covering the spectral region 0–20 nm. At 45° to the laser beam axis a second transmission grating spectrometer (TGSac, off-axis) is installed (grating 10 000 l/mm, resolution $\lambda/\Delta\lambda = 300$ at 13 nm, comparable to those described in [19]), which is calibrated in absolute terms in the wavelength range between 10 nm and 15 nm at the synchrotron facility BESSY II (beamline of the Physikalisch Technische Bundesanstalt) and is used to calibrate secondarily also the first TGS. Spectra are registered with backilluminated thinned 512×512 pixel CCD X-ray cameras (Photometrics, Scientific Instruments). Optical light is blocked with 200 nm Zr filters. In order to avoid artefacts from residual optical or scattered EUV-light each spectrum is corrected with an adjacent background trace from the respective CCD photo. We integrated the spectra over 9 laser shots for quantitative analysis.

In order to characterize the Xe-cluster target a Rayleigh scattering technique was employed with a doubled laser frequency $2\omega_0$ (400 nm) beam having a pulse energy of 100 μJ and a pulse width of 200 ps. The scattered signal S in dependence from the backing pressure p_0 scaled in our measurement with $S \sim p_0^{1.9}$ [16]. A quantitative estimation of the cluster size based on scattered photon numbers gives about $(1-5)\times 10^6$ atoms/cluster [20] for 20 bar backing pressure. Assuming 100% condensation into clusters and a linear relation between cluster number and backing pressure [5] we would expect cluster sizes of $(3-10) \times 10^5$ atoms at 5 bar and of $(2-8) \times 10^6$ atoms at 50 bar. An estimation of the expansion of the heated plasma region and the produced free electron density at maximum EUV yield was carried out with an interferometer experiment similar to Ditmire *et al.* [21] and a respective calculation technique [22]. For this purpose a part of the heating 2 ps laser beam was frequency doubled and transmitted *via* an optical delay line through the target region at right angle to the main focused beam. From the interferogramms a 240 μm extension of the plasma was inferred which is larger than the width of the optical focus. That might be already due to ionization in the wings of the laser intensity distribution. Taking this object size and the measured fringe shift an average electron density in the plasma region of about 10^{18} cm^{-3} is calculated.

The laser absorption behavior of the gas cluster target at the relevant heating laser intensities was deduced from a measurement of the laser energy transmitted through the target as a function of the backing pressure. Figure 1 shows that the cluster target forms a dense object for powerful optical femtosecond and picosecond laser pulses [5]. At already low pressures with the onset of cluster formation a sharp decrease in the transmission of the heating laser beam through the cluster target occurs due to enhanced laser light absorption because back and side scattering seems not to be predominant [4]. These obtained

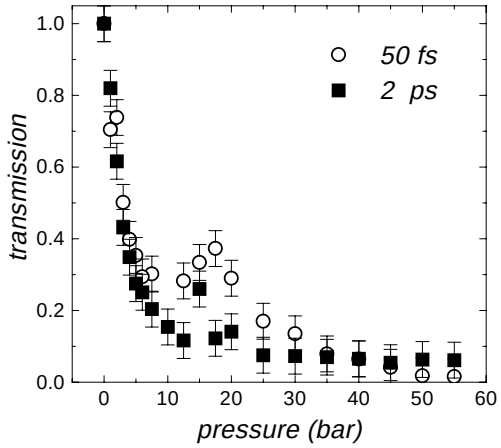

Fig. 1. Measured transmission of the Xe-cluster target in dependence from Xe backing pressure at focused intensities of 2×10^{18} W/cm^2 (50 fs) and 5×10^{16} W/cm^2 (2 ps), respectively.

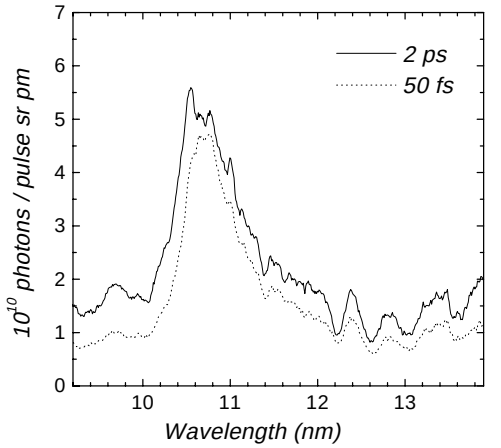

Fig. 2. Spectra registered with the off-axis TGS (calibrated in absolute terms) for 2 ps (20 bar Xe backing pressure) and 50 fs (15 bar Xe backing pressure) laser pulses (200 mJ).

characteristics will be related to the EUV-emission results discussed in the following.

In general three broadband emission peaks were observed within a (1–16) nm wavelengths range depending on the backing pressure. Emission from Xe-ions in this broad range is attributed to ionization stages up to Xe XXX [23]. This work focuses on emission between 10 nm and 14 nm which is well-known to give emission peaks from Xe^{9+} to Xe^{11+} ions [24]. In Figure 2 we depict spectra from the off-axis spectrometer obtained with the two different excitation pulse widths whereas the backing pressure was chosen for maximum photon yield. A slightly enhanced emission covering a factor of 1.3±0.2 is visible in the whole spectral range for the 2 ps laser driver pulses. This corresponds also to the observed transmission characteristic of Figure 1 which would imply a somewhat higher absorption of the 2 ps pulses in the pressure range between 7 bar and 25 bar. But probably the transmission characteristic can not display the complete absorption and related EUV-emission behavior especially at high pressures when

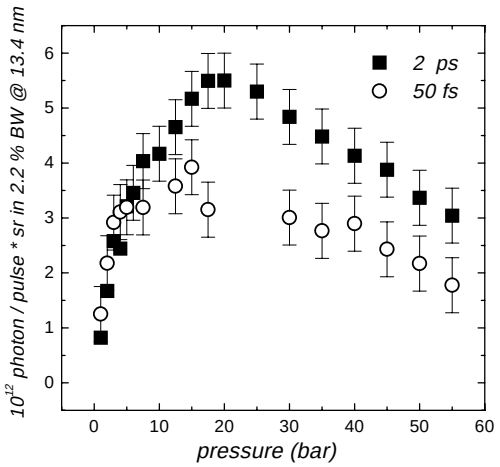

Fig. 3. Emitted photon number (off-axis) at 13.4 nm in dependence of Xe backing pressure and different laser pulse widths (*cf.* Fig. 2).

the target becomes opaque. In Figure 3 this circumstance is visible in the pressure dependent emission at 13.4 nm, a wavelength for which high quality EUV-optical components have been developed. Also at backing pressures above 30 bar a slightly higher emission signal results from a 2 ps laser pulse compared to a 50 fs laser pulse at similar pressure values. The influence of the driving laser pulse width as well as the cluster size for Xe-plasma production and related EUV-emission can be discussed in context with the Xe-cluster disassembly time. In case of our relevant cluster sizes hydrodynamic expansion is predominant and the cluster expansion time τ_{ex} is approximately [5]

$$\tau_{\mathrm{ex}} \approx r_{\mathrm{c}}(m_{\mathrm{i}}/(ZkT_{\mathrm{e}}))^{1/2}(n_{\mathrm{c}}/n_{\mathrm{s}})^{1/3}, \qquad (1)$$

where r_{c}, n_{c} is the initial cluster radius and density, respectively, n_{s} is the surrounding ambient average gas density, kT_{e} is the cluster electron temperature and Z is the average charge per ion with a mass m_{i} in the cluster. In case of a Xe-cluster with a 40 nm diameter ($\sim 10^6$ atoms/cluster) and heated to an initial electron temperature of $kT_{\mathrm{e}} = 1\,000$ eV [25] one obtains an expansion time of $\sim$ 6 ps. Increased cluster size increases the laser light absorption because the ions in the cluster hold together for a longer time and favoring thus energy transfer processes which act efficiently at high electron and ion densities. Enhanced absorption results in enhanced EUV-emission as depicted in Figure 3. The heating laser pulse width dependence suggests that the energy transfer is efficient if the pulse width matches the ps-scale of the cluster disassembly. This emphasizes the governing role of collisional processes like inverse bremsstrahlung and stimulated Raman scattering [5] which are much more significant in clusters compared to atomic gas ensembles. For the somewhat advantageous use of ps- instead of fs-pulses the cluster size should be slightly larger in order to give the optimum energy conversion. This tendency is somewhat visible in a slight different position of the emission maxima in Figure 3. However effects with increasing backing pressure run against the strong absorption of Xe at 13 nm because the heated plasma region is located in an ambient Xe-cluster gas. This affects emission maxima and signal decrease. The ps-driver pulses resulted in a similar spatial EUV-emission registered with both spectrometers. Contrary the heating with fs-pulses yielded an up to three times enhanced emission in on-axis direction compared to off-axis direction at Xe backing pressures up to 10 bar. We would assume that this fact could be connected with a much higher asymmetry of the created plasma object related to the ratio of the laser beam waist and Rayleigh range when ultrashort laser pulses are used which could be an interesting feature for further studies on future cluster based ASE (amplified spontaneous emission) sources. In contrast a ps-pulse heats also during plasma expansion which seems to tend to smooth already the plasma distribution.

Before collisional heating of the laser plasma can occur an initial ionization of the system has to take place. Optical field ionization is the relevant process if high intensity ($> 10^{15}$ W/cm^2) ultrashort laser pulses are applied. For our focal intensities 5×10^{16} W/cm^2 and more than ever 2×10^{18} W/cm^2 the ionization rates [26] from Xe I to Xe XII are several orders of magnitude higher than an estimated maximum collisional ionization rate from Xe X to Xe XII which is in a range of $10^9 ... 10^{10}$ s^{-1} [27]. From theoretical considerations, however, EUV spectra generated with linearly and elliptically polarized laser light should show a significant difference due to resulting higher energies of electrons field ionized with circularly polarized light [28]. Up to now experiments have verified this mechanism in low density gas targets, where other heating mechanisms are ineffective. Contrary to this in case of high density gas jets or in cluster targets the initial field ionization is followed by further collisional processes which in turn modify the ionic state distribution and can act back to the laser beam distribution [28].

Circularly polarized laser light was produced by inserting a $\lambda/4$-plate in the beam. In Figure 4 the plotted energy conversion efficiency from a 2 ps laser pulse into 13.4 nm radiation shows the difference for the two different polarization states. In the whole range of relevant Xe backing pressures the emission around 13.4 nm is about 2 times higher if circularly instead of linearly polarized light is used. At 15 bar the ratio is about three. The same feature was registered for the whole (10–15) nm emission range and also for fs-pulse excitation.

Within a 2.2 % bandwidth centered at 11.4 nm and 13.4 nm the total integrated off-axis flux in relation to the incident laser energy (conversion efficiency $\equiv$ CE) is summarized in Table 1. At these wavelengths Mo:Be (11.4 nm) and Mo:Si (13.4 nm) multilayer mirrors can be provided with high reflectivity (>50%). The emission was extrapolated in 2π sr solid angle using the observation angle of 0.05 msr of the off-axis spectrometer. In case of fs-laser driver pulses the off-axis and on-axis data have been averaged. Moreover integrating the wavelength region from 10 nm to 15 nm a CE of up to 7.5% (fs-pulse) and 12% (ps-pulse) in 2π sr has been achieved. From experiments where Xe-cluster targets were irradiated by KrF laser pulses with

Table 1. Maximum achieved conversion efficiencies with different laser parameters from Xe-cluster targets.

	11.4 nm		13.4 nm	
laser pulse duration and polarization	conversion efficiency in %, on 2π sr, in 2.2% BW	pressure (bar)	conversion efficiency in %, on 2π sr, in 2.2% BW	pressure (bar)
50 fs, linear	0.3	15	0.2	15
50 fs, circular	0.7	10	0.5	10
2 ps, linear	0.4	20	0.3	20
2 ps, circular	1.05	15	0.8	15

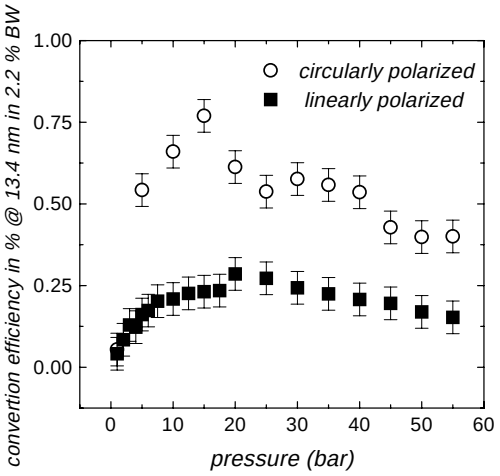

Fig. 4. Conversion efficiency at 13.4 nm related to recorded off-axis EUV-emission and incident laser energy E_{L} at different Xe backing pressure when linearly (E_{L} = 180 mJ) and circularly (E_{L} = 75 mJ) polarized 800 nm laser light with a pulse duration of 2 ps is used for excitation. (It was verified that the change of laser energy in this range did not affect the conversion efficiency.)

100 fs pulse length [13] CEs of 0.18%/sr at (11 ± 0.27) nm and up to 1.1%/sr in the region from 5 nm to 20 nm have been reported. A specially designed Xe-gas source has yielded a CE of 0.2%/(1% bandwidth (BW) 2π sr) at 12.8 nm by applying a 28 ns pulsed KrF-laser [29]. Our CE of 0.8% at 13.4 nm is slightly above to these values and similar to the related value given by Tichenor *et al.* [30] who has found for ns irradiated Xe cluster/microdroplet-targets (*cf.* comment in [12]) a CE of about 0.7% in 2π sr and 2.2% BW. In contrast, for a Xe jet-target irradiated by YAG laser pulses of 10 ns duration CEs were reported [31] of 0.6% in 2π sr and 0.2% in 2π sr at 11.4 nm (1% BW) and 13.4 nm (2% BW), respectively.

Summarizing, xenon plasmas can provide sufficient flux in a currently desired EUV-wavelength range preset by available reflective optics. In dependence on the Xe-state of aggregation (gas, cluster, liquid) suitable laser parameters for excitation can be found in accordance to relevant plasma dynamics [12]. We investigated the optimization of EUV-yield from Xe-clusters with driving laser pulses matched to its disassembly time and obtained conversion efficiencies up to 0.8% at 13.4 nm in 2.2% bandwidth and 2π sr. Requirements from applications using the EUV-radiation and technological constraints will determine which suitable laser system and target combination can be accessed. In respect to solids rare gas clusters are low debris targets which are suited for excitation by short pulse lasers for which a rapid development of compact systems takes place. In context with other important questions regarding laser driven cluster sources as *e.g.* absorption of the ambient gas, release of high energetic ions, source size and scalability to kHz repetition rates further investigations will show up to which extent the high conversion efficiency of a Xe-cluster based EUV source can be used.

A part of this work was supported by BMBF–project 13N7784. We thank A. Egbert (LZH Hannover) and C. Reinhardt (U. Hannover) for setting up partly the Rayleigh scattering and interferometry experiments and W. Karpov for laser operation.

References

1. *Emerging Lithography Technologies IV*, Proc. SPIE **3997** (2000).
2. H. Kondo, T. Tomie, H. Shimizu, Appl. Phys. Lett. **72**, 2668 (1998).
3. *X-ray Microscopy and Spectromicroscopy*, edited by J. Thieme, G. Schmahl, D. Rudolph, E. Umbach (Springer, Heidelberg, 1998).
4. T. Ditmire, R.A. Smith, J.W.G. Tisch, M.H.R. Hutchinson, Phys. Rev. Lett. **78**, 3121 (1997).
5. T. Ditmire, T. Donnelly, A.M. Rubenchik, R.W. Falcone, M.D. Perry, Phys. Rev. A **53**, 3379 (1996).
6. A. McPherson, B.D. Thompson, A.B. Borisov, K. Boyer, C.K. Rhodes, Nature **370**, 631 (1994).
7. T. Ditmire, J.W.G. Tisch, E. Springate, M.B. Mason, H. Hay, R.A. Smith, J. Marangos, M.H.R. Hutchinson, Nature **386**, 54 (1997).
8. M. Lezius, S. Dobosz, D. Normand, M. Schmidt, Phys. Rev. Lett. **80**, 261 (1998).
9. K. Boyer, B.D. Thompson, A. McPherson, C.K. Rhodes, J. Phys. B. At. Mol. Opt. Phys. **27**, 4373 (1994).
10. D. Stearns, R. Rosen, S. Vernon, Appl. Opt. **32**, 6952 (1993).
11. K. Skulina, C. Alford, R. Bionta, D. Makowieki, E. Gullikson, R. Soufli, J. Kortright, J. Underwood, Appl. Opt. **34**, 3727 (1995).
12. E. Parra, I. Alexeev, J. Fan, K.Y. Kim, S.J. McNaught, H.M. Milchberg, Phys. Rev. E **62**, R5931 (2000).
13. E. Miura, H. Honda, K. Katsura, E. Takahashi, K. Kondo, Appl. Phys. **70**, 783 (2000).

14. D.A. Tichenor, A.K. Ray-Chaudhuri, W.C. Replogle, R.H. Stulen, G.D. Kubiak, L.E. Klebanoff, J.B. Wronosky, L.C. Hale, H.N. Chapman, J.S. Taylor, Proc. SPIE **4343**, (2001, in press).
15. P.V. Nickles, M. Kalachnikov, P.J. Warwick, K.A. Janulewicz, W. Sandner, U. Jahnke, D. Hilscher, M. Schnürer, R. Nolte, A. Rousse, Quant. Electron. Russia **29**, 444 (1999).
16. S. Ter-Avetisyan *et al.*, Phys. Rev. E (submitted).
17. T. Auguste, P.D. Oliveira, S. Hulin, P. Monot, J. Abdallah Jr, A.Ya. Faenov, I.Yu. Skobolev, A.I. Magunov, T.A. Pikuz, JETP Lett. **72**, 38 (2000).
18. O.F. Hagena, W. Obert, J. Chem. Phys. **56**, 1793 (1972); O.F. Hagena, Rev. Sci. Instrum. **63**, 2374 (1992).
19. T. Wilhein, S. Rehbein, D. Hambach, M. Berglund, L. Rymell, H.M. Hertz, Rev. Sci. Instrum. **70**, 1694 (1999).
20. The large uncertainty comes from the average density number estimation in the interaction zone and further specifics of this method, see A.J. Bell *et al.*, J. Phys. D: Appl. Phys. **26**, 994 (1993).
21. T. Ditmire, R.A. Smith, Opt. Lett. **23**, 619 (1998).
22. Software IDEA, M. Hipp, P. Reiterer, Technical University Graz, Austria.
23. H. Honda, E. Miura, K. Katsura, E. Takahashi, K. Kondo, Phys. Rev. A **61**, (2000); B.A.M. Hansson, L. Rymell, M. Berglund, H.M. Hertz, Microel. Engin. **53**, 667 (2000).
24. J. Blackburn, P.K. Carroll, J. Costello, G. O'Sullivan, JOSA **73**, 1325 (1983).
25. Y.L. Shaö, T. Ditmire, J.W.G. Tisch, E. Springate, J.P. Marangos, M.H.R. Hutchinson, Phys. Rev. Lett. **77**, 3343 (1996).
26. N.H. Burnett, P.B. Corkum, JOSA B **6**, 1195 (1989).
27. W. Lotz, Z. Phys. **216**, 241 (1968).
28. E.E. Fill, JOSA B **11**, 2241 (1994); P.B. Corkum, N.H. Burnett, F. Brunel, Phys. Rev. Lett. **62**, 1259 (1989).
29. R. de Bruijn, A. Bartnik, H. Fledderus, H. Fiedorowicz, P. Hegeman, R. Constantinescu, F. Bijkerk, Proc. SPIE **3997**, 157 (2000).
30. D.A. Tichenor, G.D. Kubiak, W.C. Replogle, L.E. Klebanoff, J.B. Wronosky, L.C. Hale, H.N. Chapman, J.S. Taylor, J.A. Folta, C. Montcalm, R.M. Hudyma, K.A. Goldberg, P. Naulleau, Proc. SPIE **3997**, 48 (2000).
31. B.A.M. Hansson, M. Berglund, O. Hembers, H.M. Hertz, Proc. SPIE **3997**, 729 (2000).